Science Advances
AAAS

Supplementary Materials for

Proton-conductive aromatic membranes reinforced with poly(vinylidene fluoride) nanofibers for high-performance durable fuel cells

Fanghua Liu *et al.*

Corresponding author: Kenji Miyatake, miyatake@yamanashi.ac.jp

Sci. Adv. **9**, eadg9057 (2023)
DOI: 10.1126/sciadv.adg9057

This PDF file includes:

Figs. S1 to S17
Tables S1 to S5

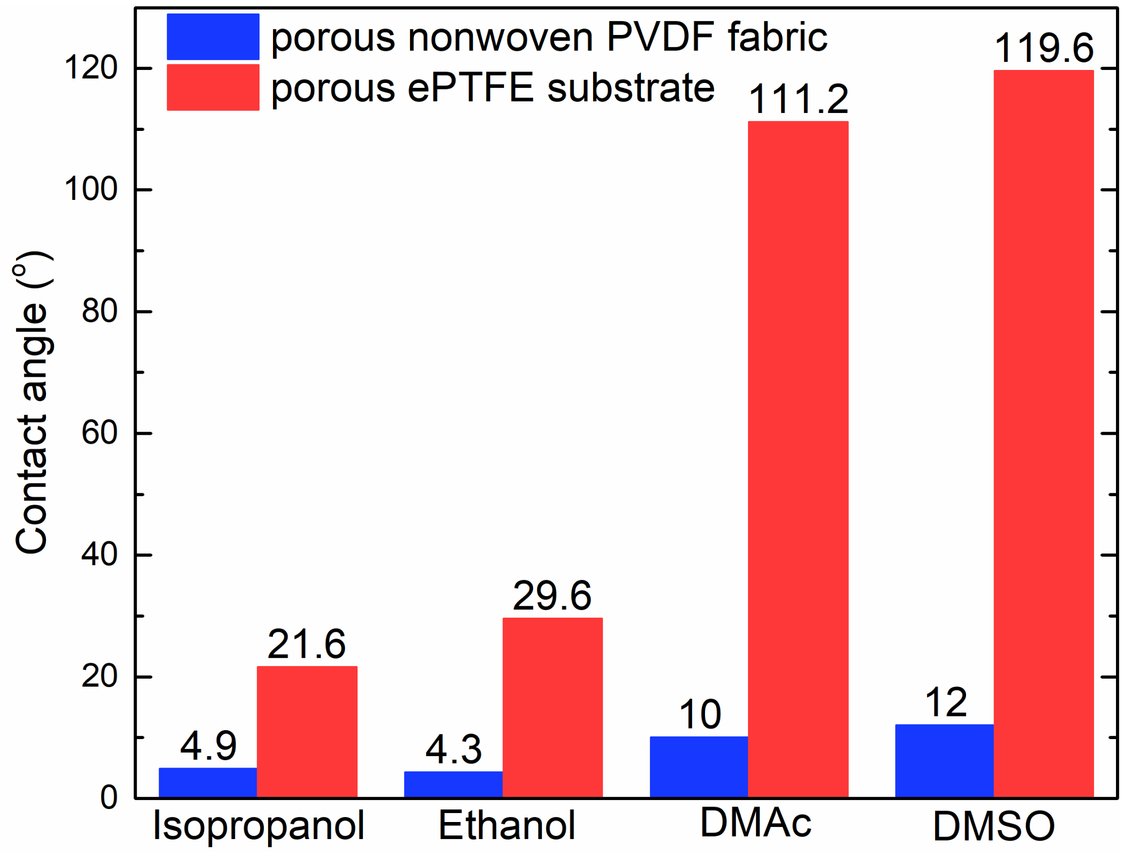

Fig. S1. Contact angles of different solvents on the porous nonwoven PVDF fabric and porous ePTFE substrate at room temperature.

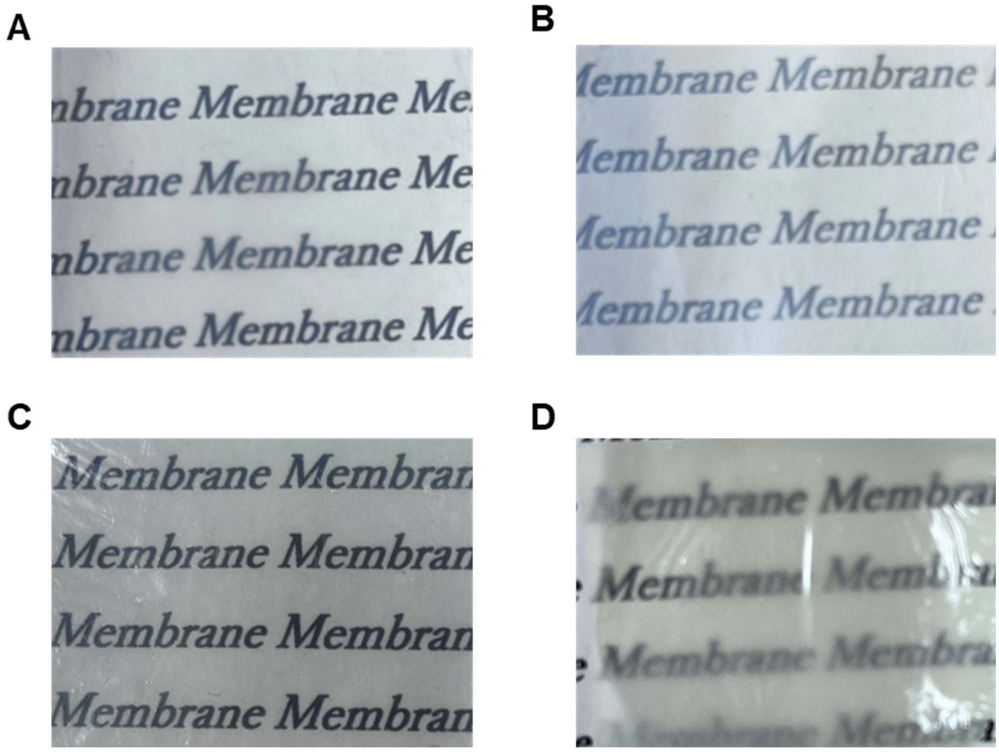

Fig. S2. Images of the reinforcement materials and reinforced membranes. (**A**) Porous nonwoven PVDF nanofiber fabric. (**B**) Porous ePTFE substrate. (**C**) Reinforced SPP-TFP-4.0-PVDF membrane. (**D**) Reinforced SPP-TFP-4.0-ePTFE membrane.

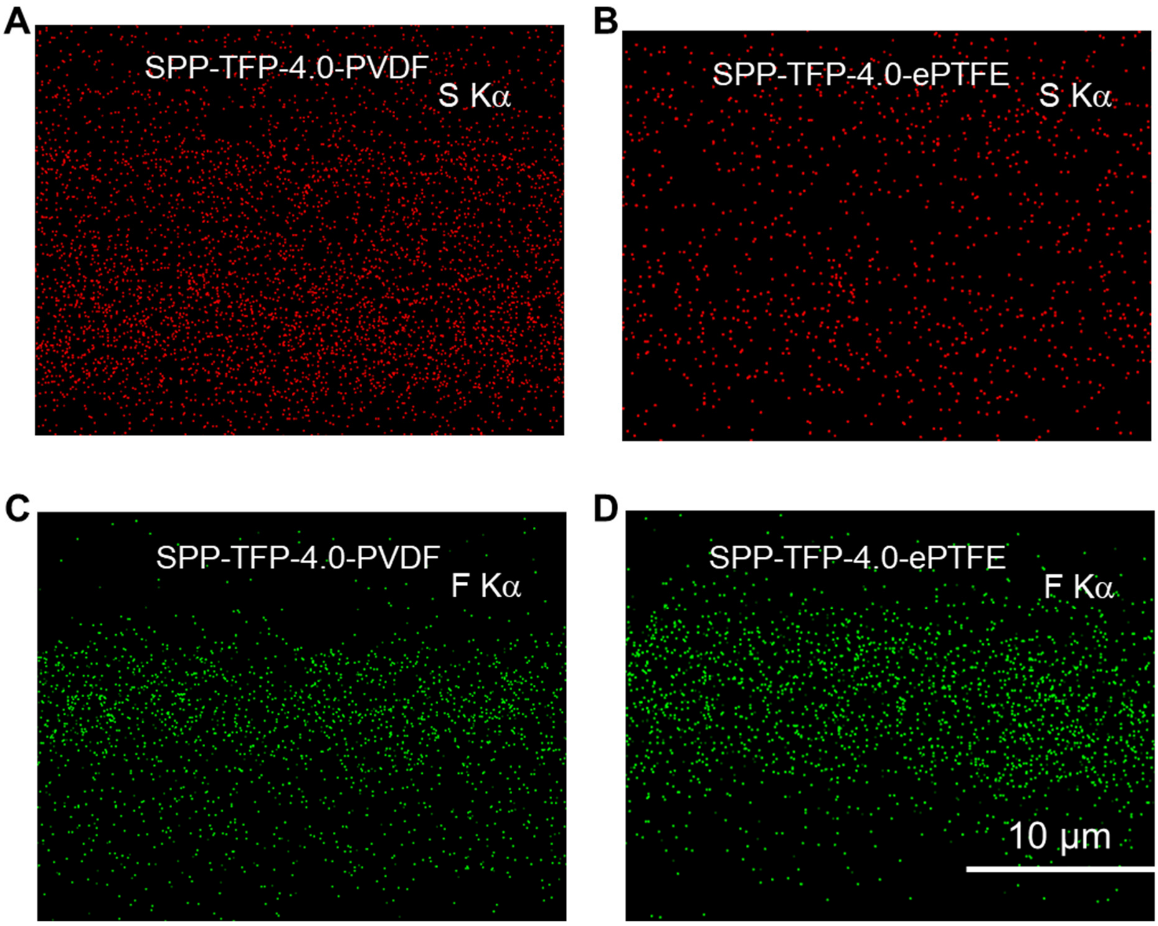

Fig. S3. Elemental mapping images of the reinforced membranes. (**A**) and (**B**) Sulfur element. (**C**) and (**D**) Fluorine element. Analyzed by EDS (energy-dispersive X-ray spectroscopy) at acceleration voltage of 15.0 kV.

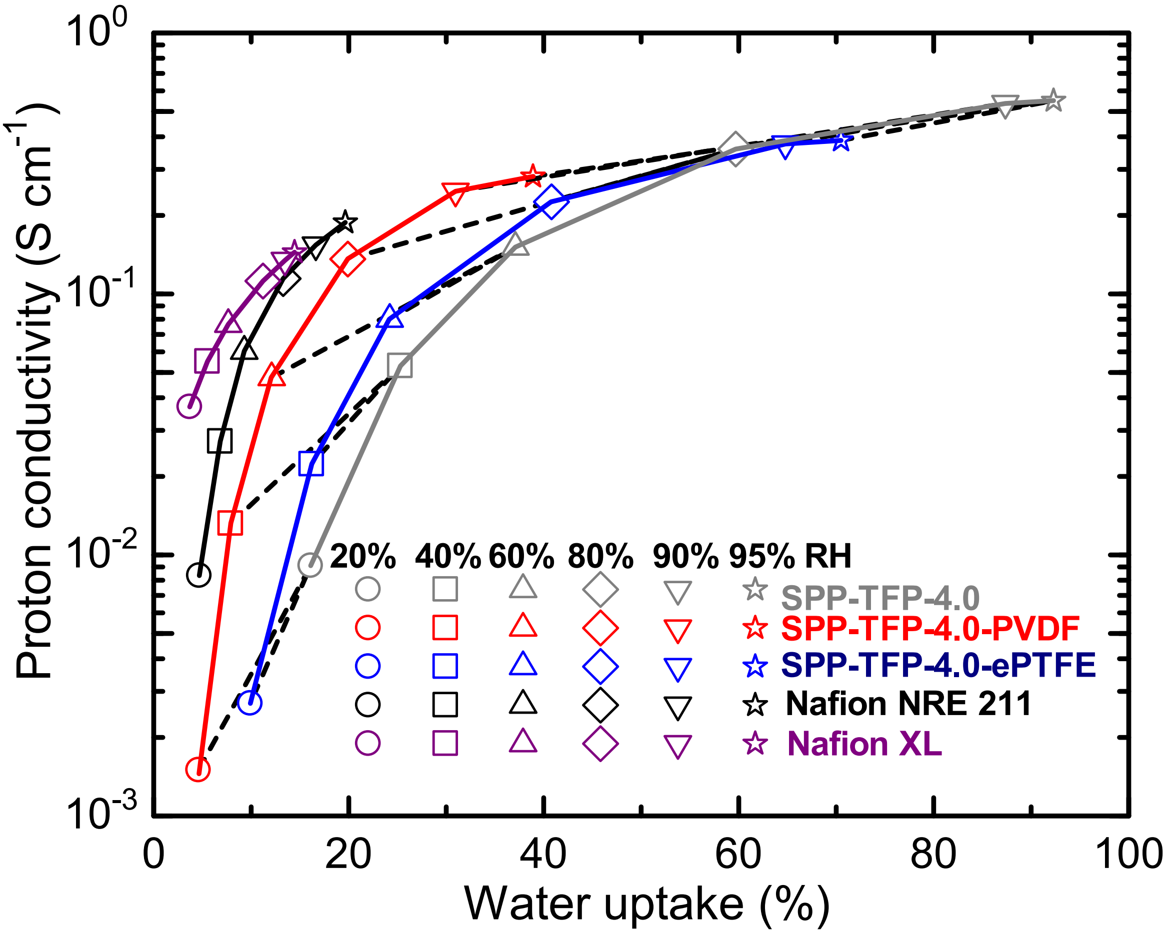

Fig. S4. Dependence of the proton conductivity on the water uptake from 20% to 95% RH at 80 °C.

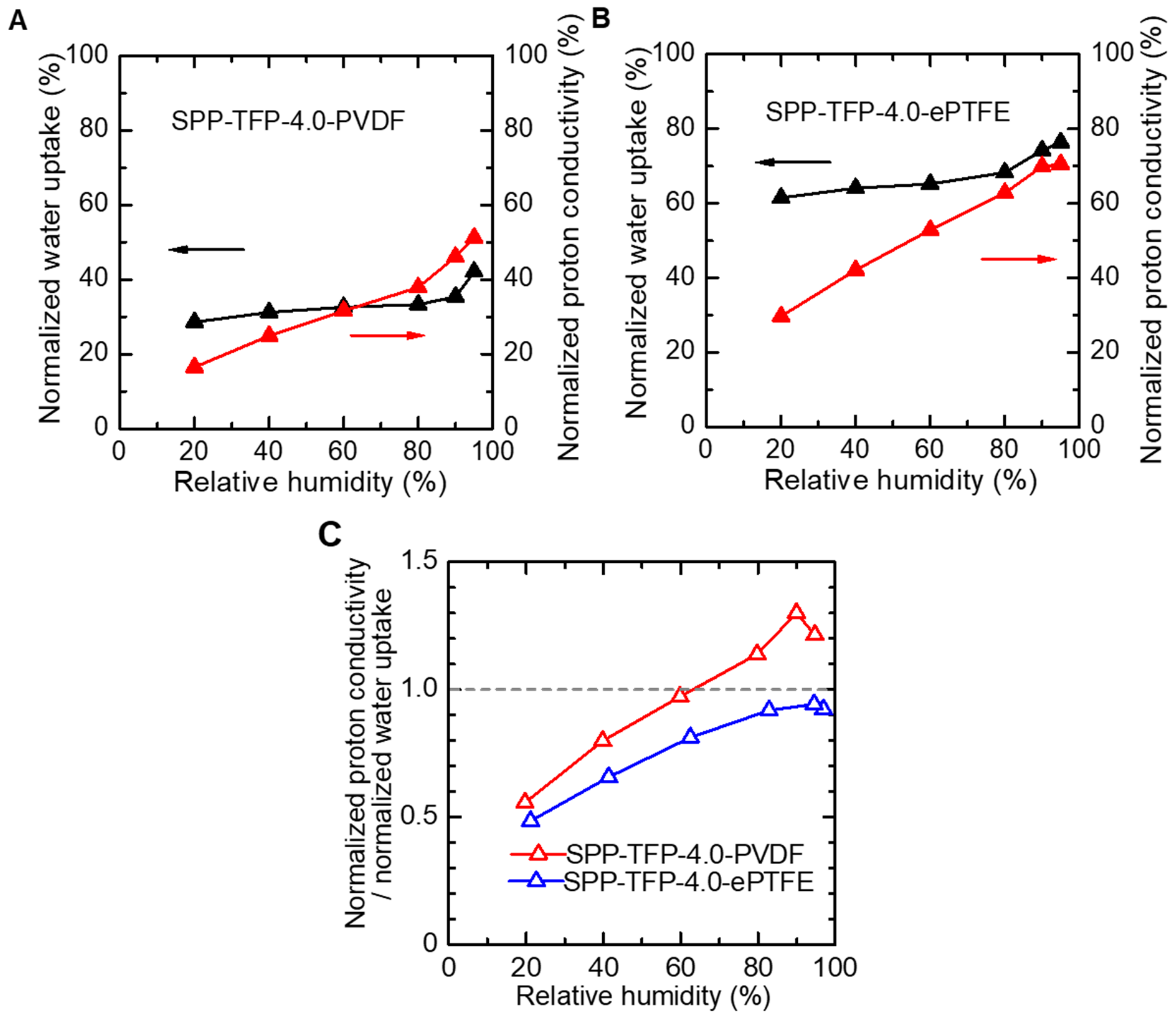

Fig. S5. The normalized water uptake and proton conductivity of reinforced membranes relative to their parent SPP-TFP-4.0 membrane under different relative humidity at 80 °C. (**A**) SPP-TFP-4.0-PVDF. (**B**) SPP-TFP-4.0-ePTFE. (**C**) Normalized proton conductivity divided by normalized water uptake as a function of relative humidity for SPP-TFP-4.0-PVDF and SPP-TFP-4.0-ePTFE.

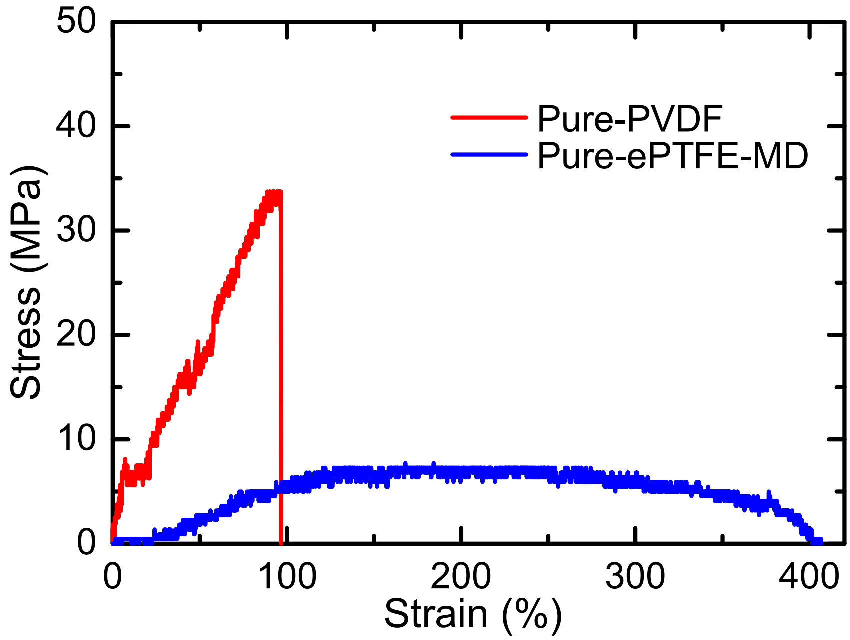

Fig. S6. Stress-strain curves of porous ePTFE substrate in machine direction (MD) and nonwoven PVDF fabric at 80 ℃ and 60% RH.

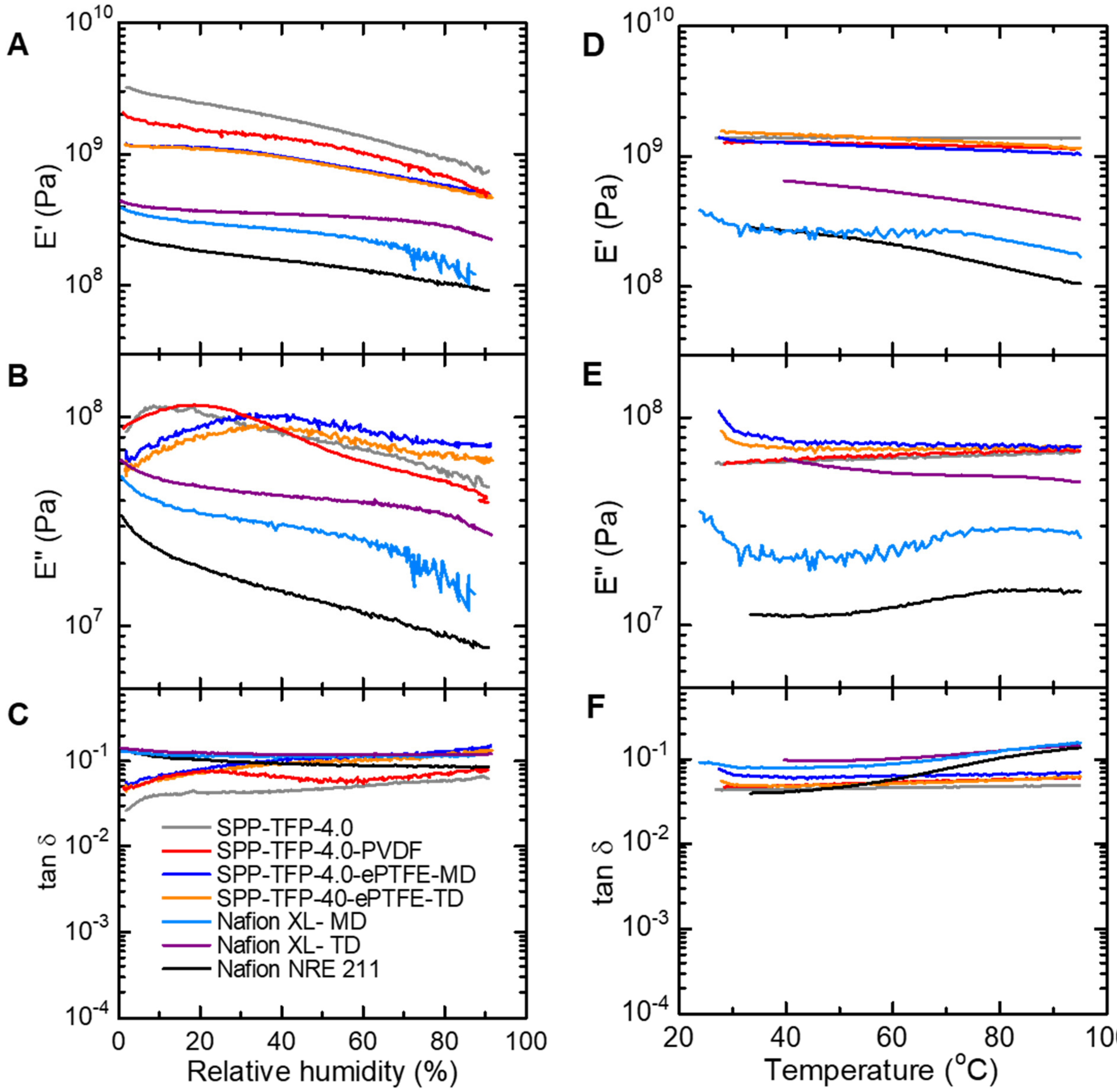

Fig. S7. The viscoelastic properties of SPP-TFP-4.0-ePTFE and Nafion XL in different directions, SPP-TFP-4.0-PVDF, parent SPP-TFP-4.0 and Nafion NRE 211. At 80 °C, relative humidity dependence of Storge modulus (E′) (**A**), loss modulus (E″) (**B**) and tan δ (=E″/E′) (**C**). At 60% RH, temperature dependence of Storge modulus (E′) (**D**), loss modulus (E″) (**E**) and tan δ (=E″/E′) (**F**).

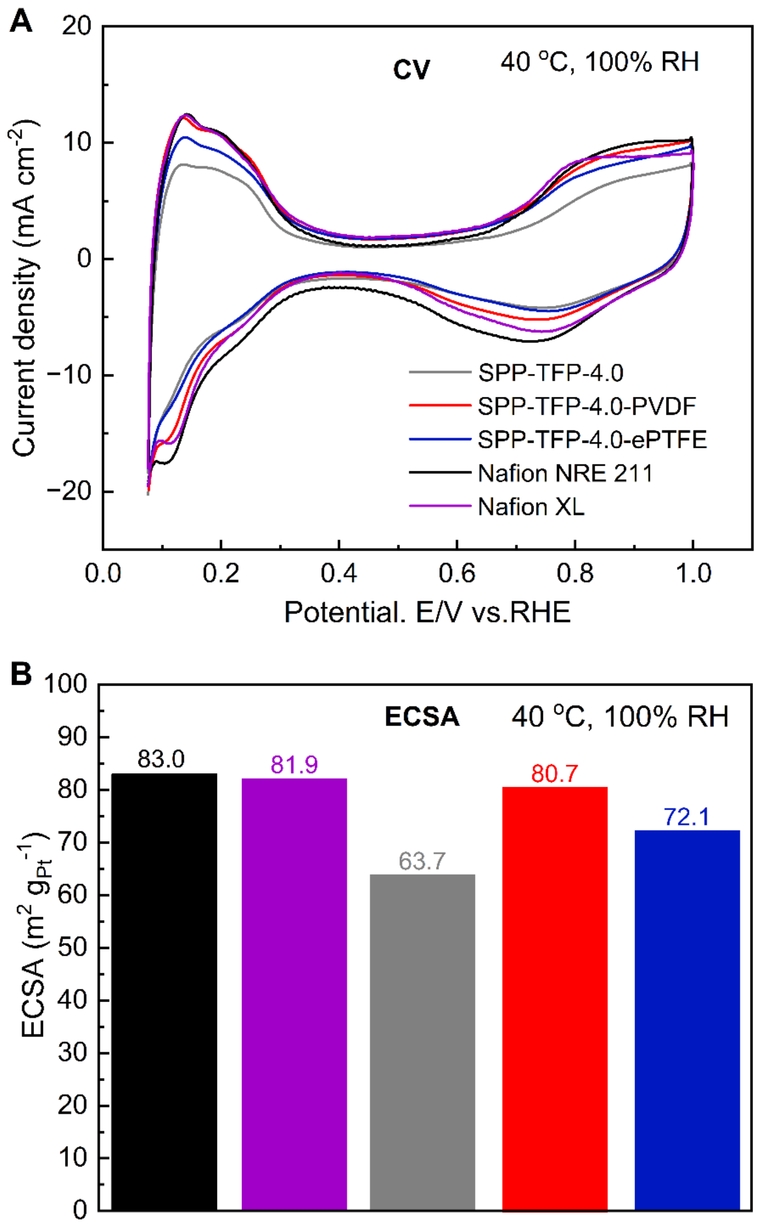

Fig. S8. CV curves with corresponding ECSA at 40 °C and 100% RH. (**A**) CV curves. (**B**) Calculated ECSA values from CV curves. The CV was obtained by sweeping the potential from 0.075 to 1.0 V vs. RHE (reversible hydrogen electrode) at a scan rate of 20 mV s^{-1} for 50 cycles, supplying hydrogen (0.1 slpm) and nitrogen (0.1 slpm) to the anode and cathode, respectively, with no back pressure. The catalyst loading was 0.5 mg cm^{-2} for all electrodes.

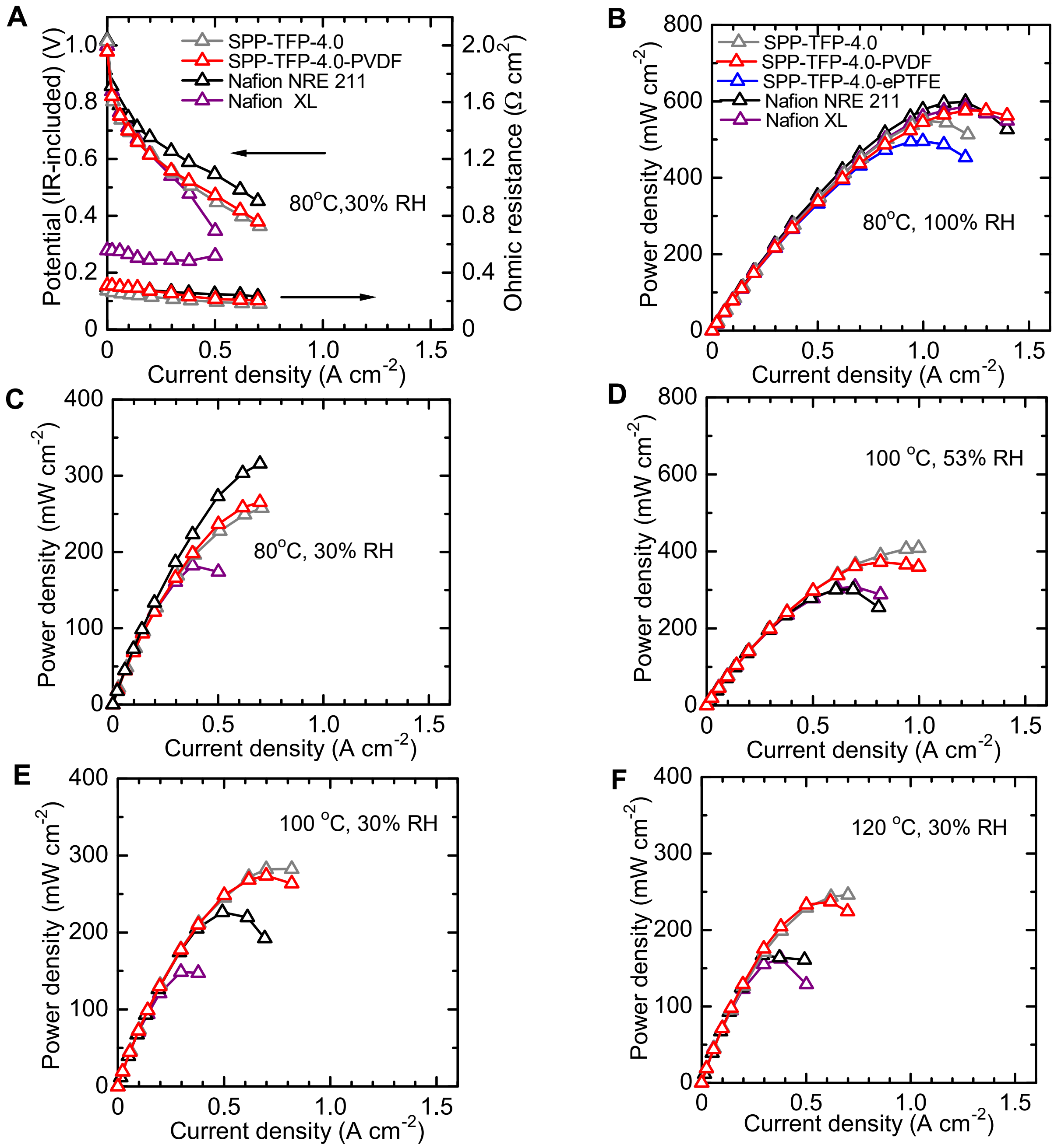

Fig. S9. Fuel cell performance. IR curves at 80 °C and 30% RH (**A**). Power density as a function of the current density at 80 °C and 100% RH (**B**), 80 °C and 30% RH (**C**), 100 °C and 53% RH (**D**), 100 °C and 30% RH (**E**), and 120 °C and 30% RH (**F**). The catalyst loading was 0.5 mg cm^{-2} for both electrodes supplying hydrogen and air to the anode and cathode, respectively, with no back pressure.

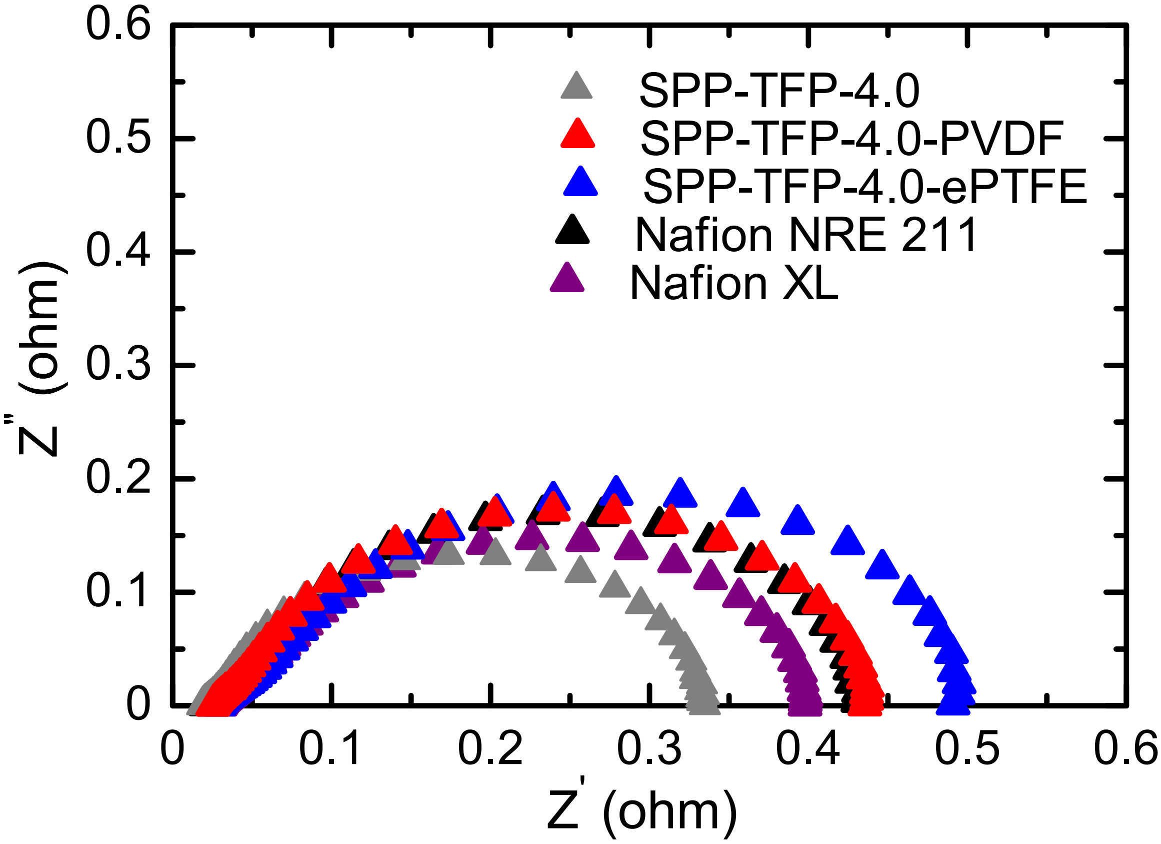

Fig. S10. Nyquist plots at 80 °C and 100% RH, feeding hydrogen (0.1 slpm) to the anode and air (0.1 slpm) to the cathode with no back pressure.

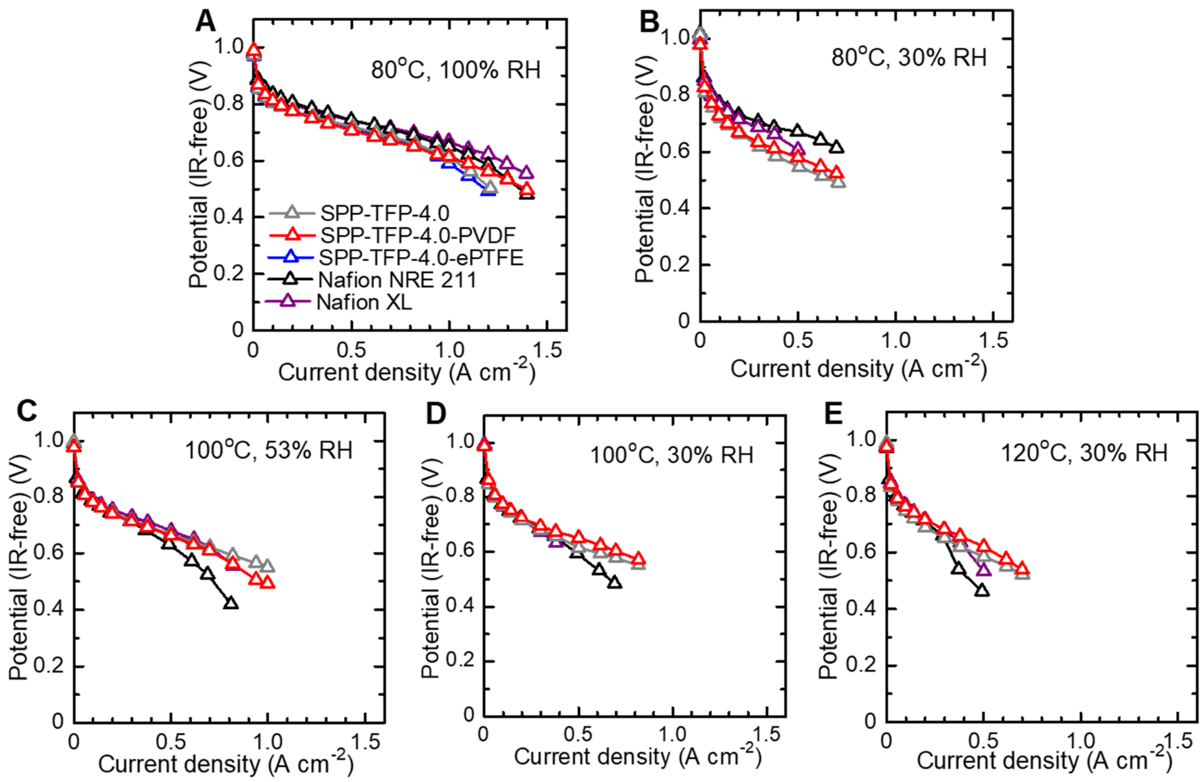

Fig. S11. IR-corrected polarization curves. (**A**) 80 °C and 100% RH, (**B**) 80 °C and 30% RH, (**C**) 100 °C and 53% RH (**D**) 100 °C and 30% RH and (**E**) 120 °C and 30% RH. The catalyst loading was 0.5 mg cm^{-2} for all electrodes supplying hydrogen and air to the anode and cathode, respectively, with no back pressure.

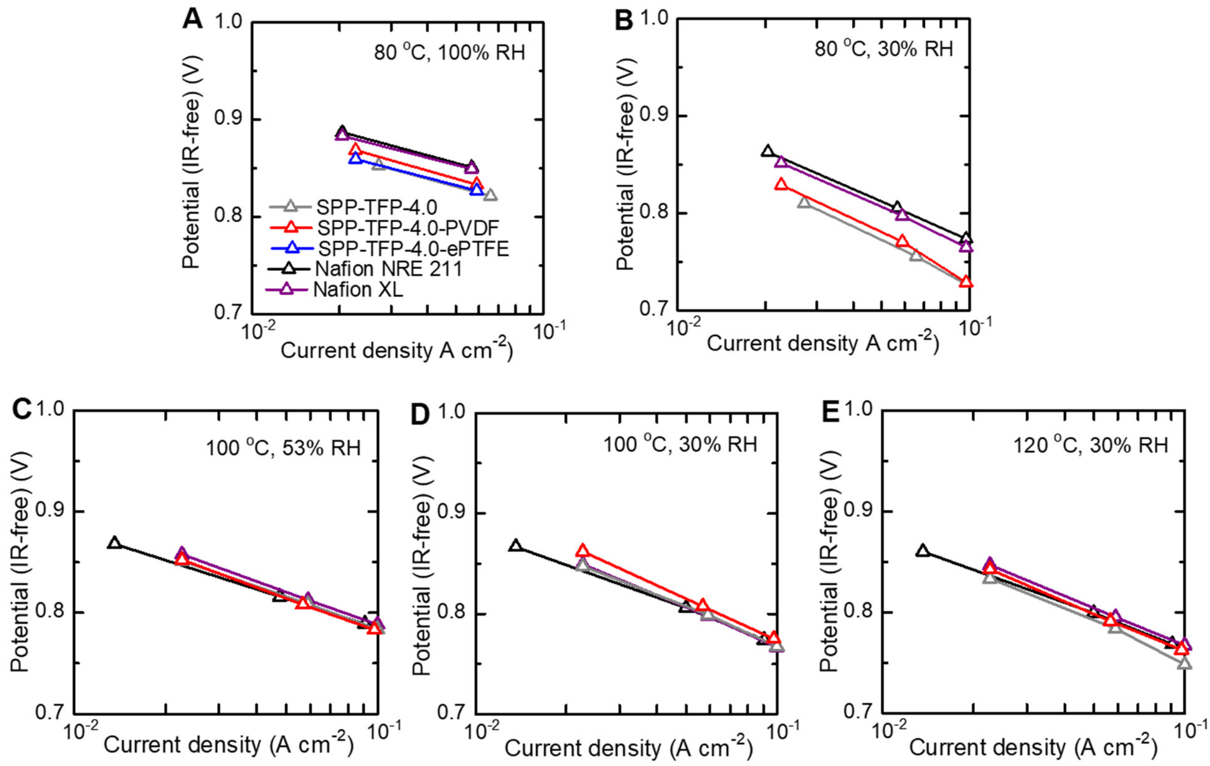

Fig. S12. Tafel curves. (**A**) 80 °C and 100% RH, (**B**) 80 °C and 30% RH, (**C**) 100 °C and 53% RH (**D**) 100 °C and 30% RH and (**E**) 120 °C and 30% RH. The catalyst loading was 0.5 mg cm^{-2} for all electrodes, supplying hydrogen and air to the anode and cathode, respectively, with no backpressure.

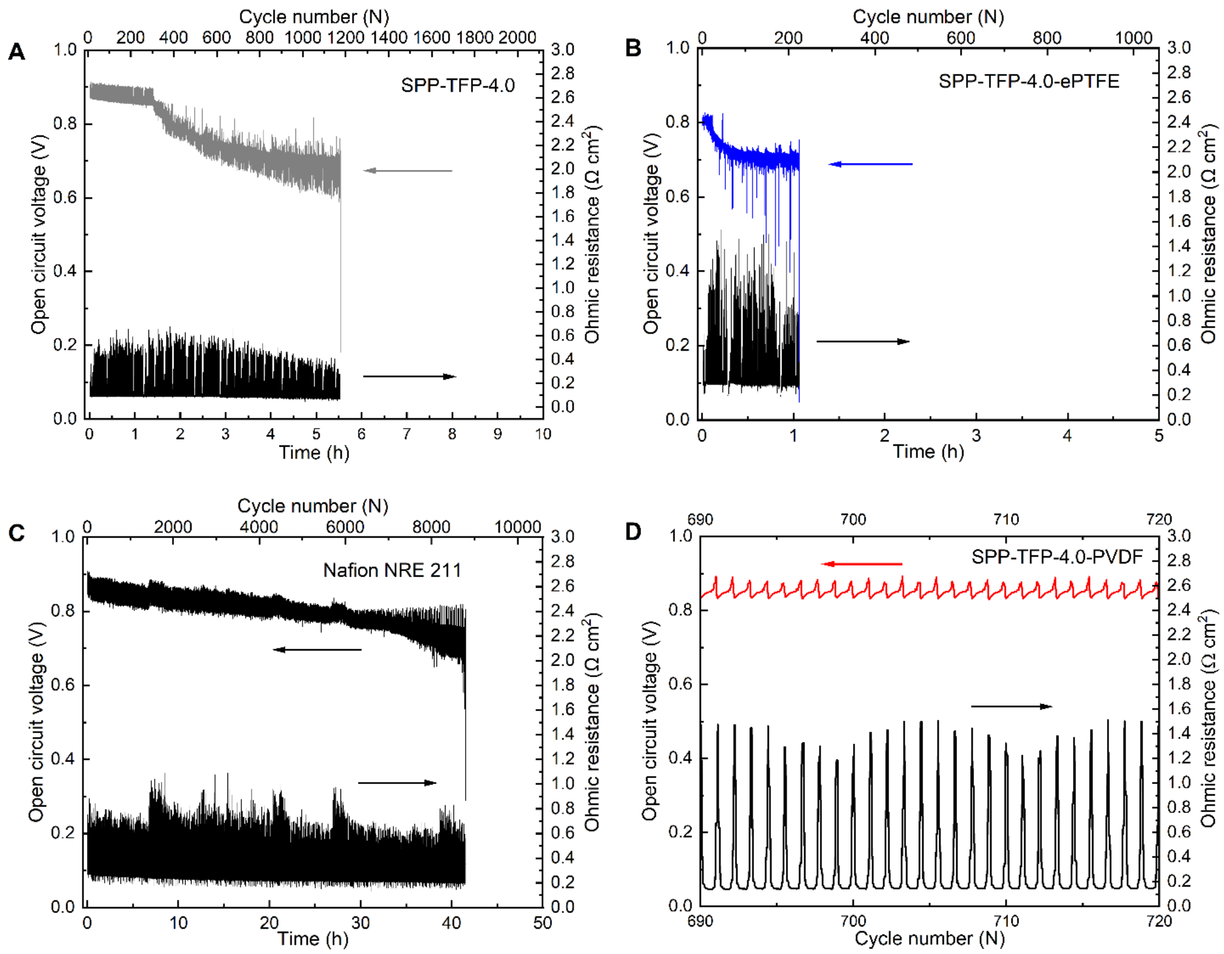

Fig. S13. Combined chemical (OCV hold) and mechanical (wet/dry cycling) durability at 90 °C without back pressure. The testing time and cycle number dependence of the OCV and ohmic resistance of SPP-TFP-4.0 (**A**), SPP-TFP-4.0-ePTFE (**B**) and Nafion NRE 211 (**C**). (**D**) Changes in OCV and ohmic resistance in each hydration regime for SPP-TFP-4.0-PVDF membrane. The tested cell loaded 0.2 and 0.1 mgPt cm^{-2} at the anode (hydrogen, 0.06 slpm) and cathode (air, 0.06 slpm), respectively. The measurement was carried out at OCV, where the frequent wet/dry cycling was conducted via switching wet gas (100% RH; 15 s) and dry gas (0% RH; 2 s).

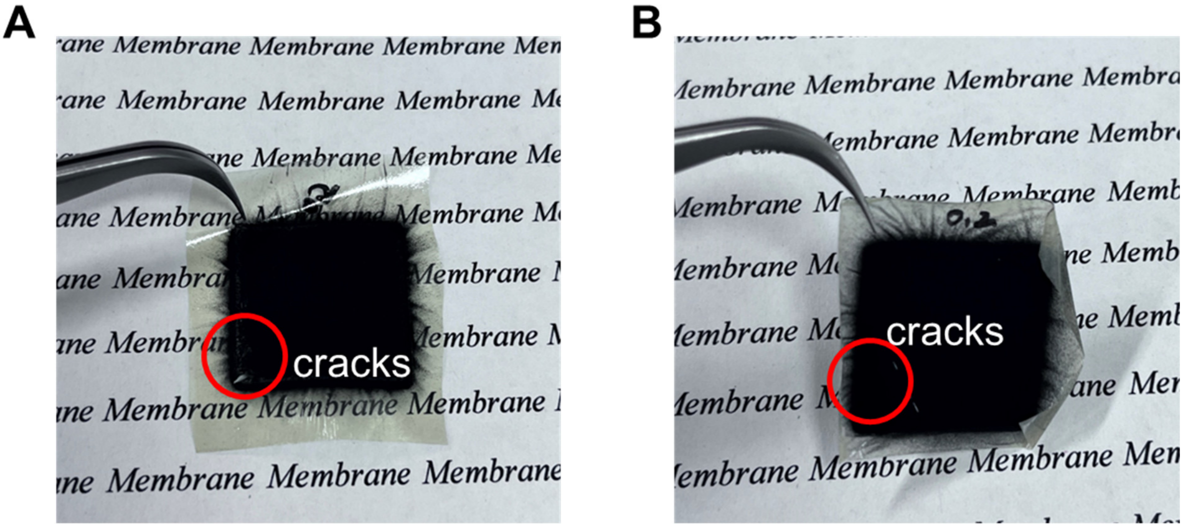

Fig. S14. The CCMs images after combined chemical and mechanical durability test. (**A**) SPP-TFP-4.0. (**B**) SPP-TFP-4.0-ePTFE.

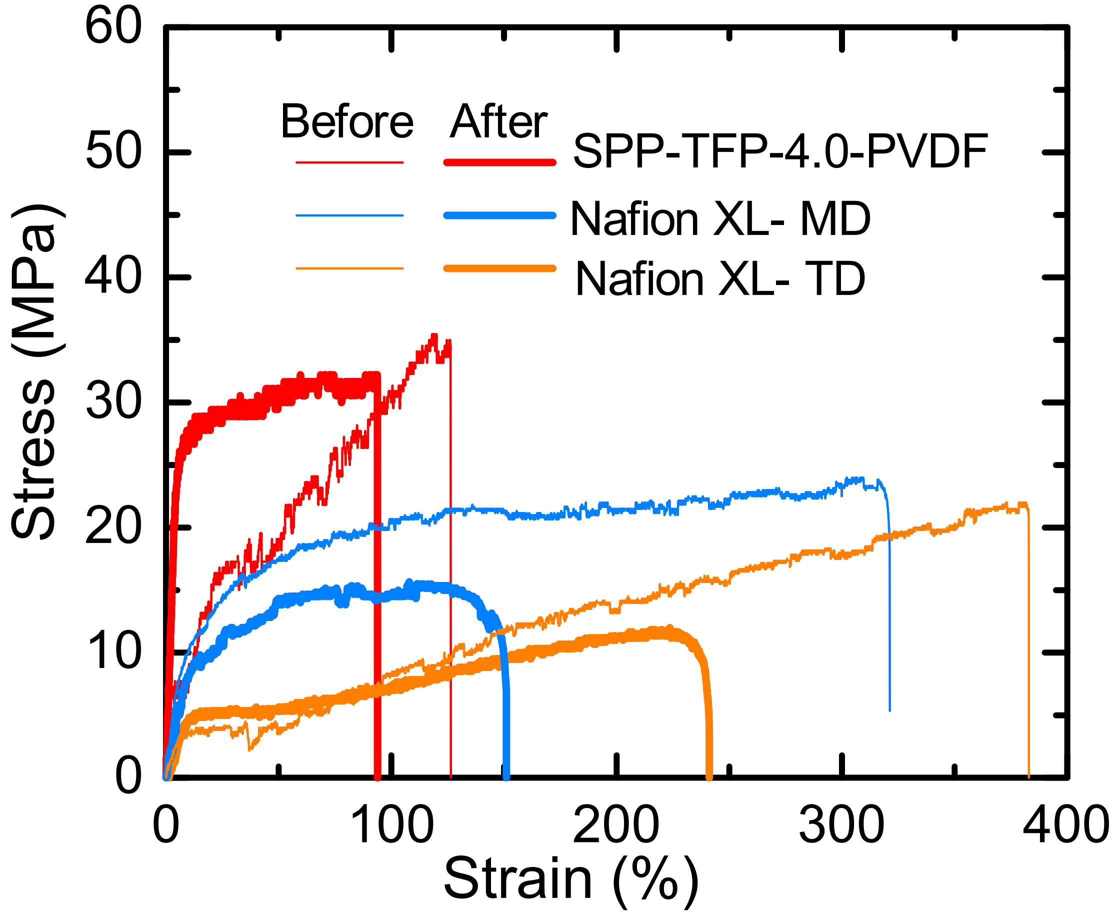

Fig. S15. The mechanical properties of SPP-TFP-4.0-PVDF and Nafion XL before and after combined chemical and mechanical durability test at 80 °C and 60% RH.

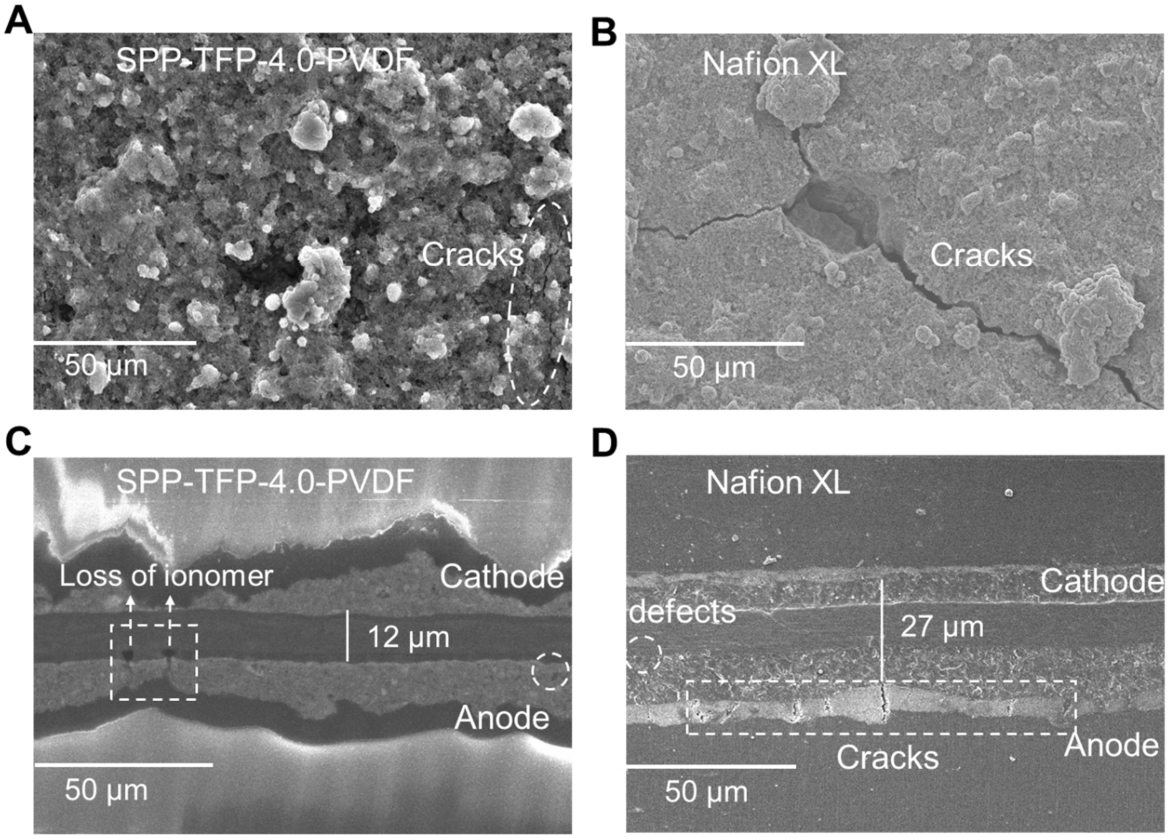

Fig. S16. The SEM images of SPP-TFP-4.0-PVDF and Nafion XL after combined chemical and mechanical durability test. (**A**) and (**B**) Surface. (**C**) and (**D**) Cross-section. A Hitachi SU3500 device was used at an accelerating voltage of 15.0 kV.

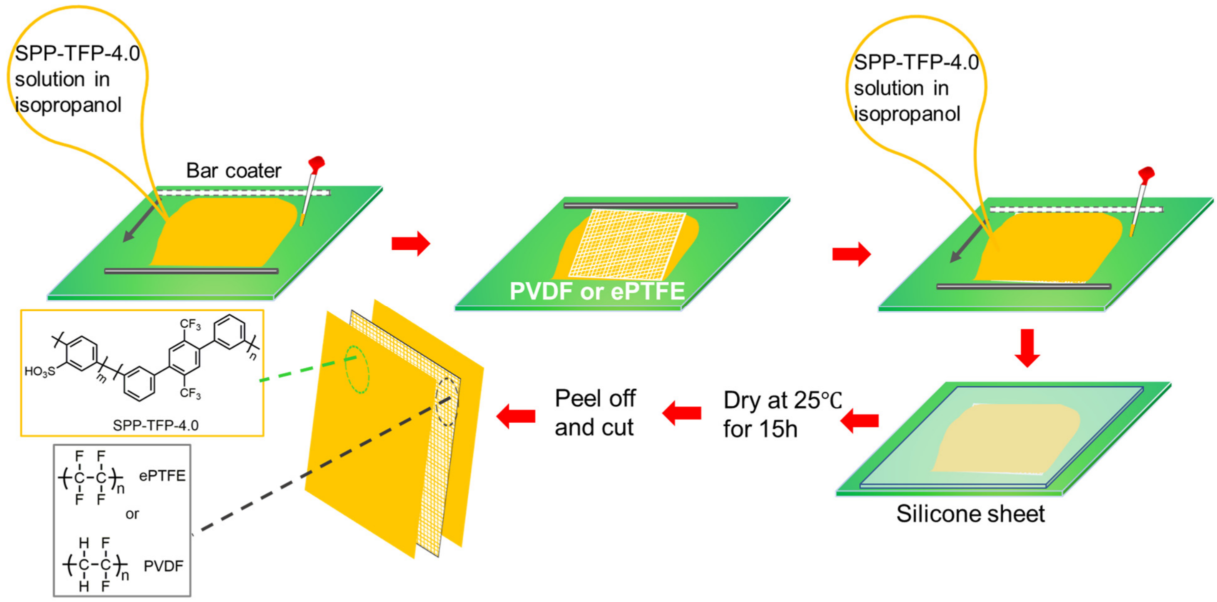

Fig. S17. Preparation process for the reinforced membranes using the push-coating method.

Table S1. The titrated IEC, hydrophilic and hydrophobic domain sizes, thickness, water uptake and swelling ratio of membranes.

Membrane	IEC (mmol g^{-1})		Domain size (nm)		Thickness (μm)	Water uptake[c] (%)		Swelling[d] at r.t. (%)	
	IEC[a]	IEC[b]	hydrophilic	hydrophobic		20% RH	95% RH	In-plane	Through-plane
SPP-TFP-4.0	--	3.40	2.50 ± 0.30	1.84 ± 0.15	27	16.1	92.3	19.9	46.6
SPP-TFP-4.0-PVDF	2.96	2.01	1.11 ± 0.24	1.93 ± 0.27	14	4.6	38.9	5.1	6.3
SPP-TFP-4.0-ePTFE	2.95	2.13	1.74 ± 0.33	1.70 ±0.20	16	9.9	70.5	13.5	14.3
Nafion NRE 211	--	0.97	--	--	25	4.7	19.7	8.5	12.0
Nafion XL	--	0.71	--	--	30	3.7	14.4	4.3	6.6

[a]: calculated from SEM images;

[b]: titrated IEC obtained by acid-base titration;

[c]: measured at 80 °C;

[d]: measured at r.t. (room temperature) in water.

Table S2. The obtained hydrogen permeability from LSV curves, and the calculated hydrogen permeability of the membranes considering the thickness and the proton conductivity at 80 °C and 100% RH.

Membrane	Thickness[a] (μm)	Hydrogen permeability[b] (mA cm^{-2})	Hydrogen permeability[c] (10^9 mmol H_2 s^{-1} cm^{-2} cm)	Proton conductivity[d] (mS cm^{-1})
SPP-TFP-4.0	27	0.90	6.3	550.1
SPP-TFP-4.0-PVDF	14	1.06	3.8	281.8
SPP-TFP-4.0-ePTFE	16	1.15	4.8	387.5
Nafion NRE 211	25	1.27	8.2	187.9
Nafion XL	30	1.07	8.3	139.5

[a]: measured by micrometer.

[b]: obtained from LSV curves at 80 °C and 100% RH;

[c]: calculated by considering the thickness of membrane;

[d]: measured at 80 °C and 95% RH.

Table S3. The test conditions and results for combined chemical and mechanical durability.

Membrane	wet/ dry time (s)	Pt loading at anode/cathode (mg cm^{-2})	OCV under wet/dry state (V)		Ohmic resistance under wet/dry state (mΩ cm^2)	Test time (h)	Cycle number (N)
			Initial	final			
SPP-TFP-4.0	15/2	0.2/0.1	0.91/0.87	0.72/0.60	0.092/0.361	5.5	1,173
SPP-TFP-4.0-PVDF	15/2	0.2/0.1	0.91/0.86	0.72/0.64	0.147/1.288	703.0	148,870
SPP-TFP-4.0-ePTFE	15/2	0.2/0.1	0.82/0.79	0.72/0.68	0.282/0.892	1.1	233
Nafion NRE 211	15/2	0.2/0.1	0.91/0.86	0.76/0.61	0.271/0.755	41.5	8,788
Nafion XL	15/2	0.2/0.1	0.91/0.86	0.86/0.31	0.241/0.613	415.6	88,008

Table S4. The mechanical properties of SPP-TFP-4.0-PVDF and Nafion XL at 80 °C and 60% RH before and after combined chemical and mechanical durability test.

Membrane	Yield stress (MPa)		Maximum strain (%)		Young's modulus (GPa)		Rupture energy (MJ m^{-3})	
	Before	After	Before	After	Before	After	Before	After
SPP-TFP-4.0-PVDF	35.5	32.2	126.4	94.0	0.50	0.55	28.1	27.4
Nafion XL-MD	24.0	15.7	321.2	151.1	0.16	0.08	64.3	19.5
Nafion XL-TD	22.0	12.0	383.0	241.2	0.06	0.05	48.8	19.3

Table S5. The physical parameters of porous substrates.

Substrate	Porosity (%)	Pore size (μm)	Fiber diameter (nm)	Thickness (μm)	Source
PVDF	78	0.2857	100	7	Shinshu University
ePTFE	85	0.4~0.7	-	11	Valqua LTD